Supporting Information

High Performance SnO_2/C Nanocomposite Cathode for Aluminum-Ion Battery

Hongyan Lu,[1,†] Yuanxin Wan,[2,1,3†] Tianyi Wang,[1] Rong Jin,[1] Peitao Ding,[1] Rong Wang,[1] Yong Wang,[2] Chao Teng,[2] Linling Li,[1] Xiaoliang Wang,[1,] Dongshan Zhou,[4,3,1,*] and Gi Xue [1]*

[1] Department of Polymer Science and Engineering, School of Chemistry and Chemical Engineering, State Key Laboratory of Coordination Chemistry, Key Laboratory of High Performance Polymer Materials and Technology, MOE, Nanjing University, Nanjing, 210093, China.
[2] School of Advanced Materials, Peking University Shenzhen Graduate School, Shenzhen, 518055, China.
[3] Sheyang Research Institute, Nanjing University, Sheyang, 224300, China.
[4] Shenzhen Research Institute, Nanjing University, Shenzhen, 518057, China.

*Correspondence and requests for materials should be addressed to D.Z. & X.W. (email: dzhou@nju.edu.cn, wangxiaoliang@nju.edu.cn).

†These authors contributed equally to this work.

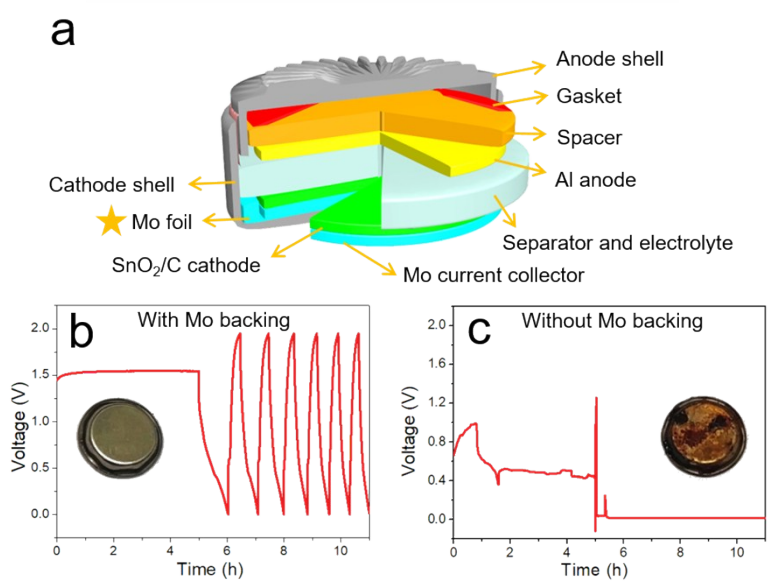

Fig. S1 a) Schematic illustration of the CR2032 coin-type cell assembly. b,c) the voltage-time curves of AIBs with and without Mo backing. All the cells were maintained for 5 hours before test. The voltage of cells with Mo backing remains 1.5 V during the initial 5 hours, while the voltage of the cells without Mo backing is fickle (range from 0.3 to 1 V) with a significant voltage decay. Insets are the photographs of cathode shells with and without Mo backing after the discharge/charge processes. The thickness of Mo foil is 20 μm. As shown clearly, the cathode shell with molybdenum foil backing is not corroded and the cell can work normally, while the cathode shell without molybdenum foil backing is strongly corroded and the cell cannot work.

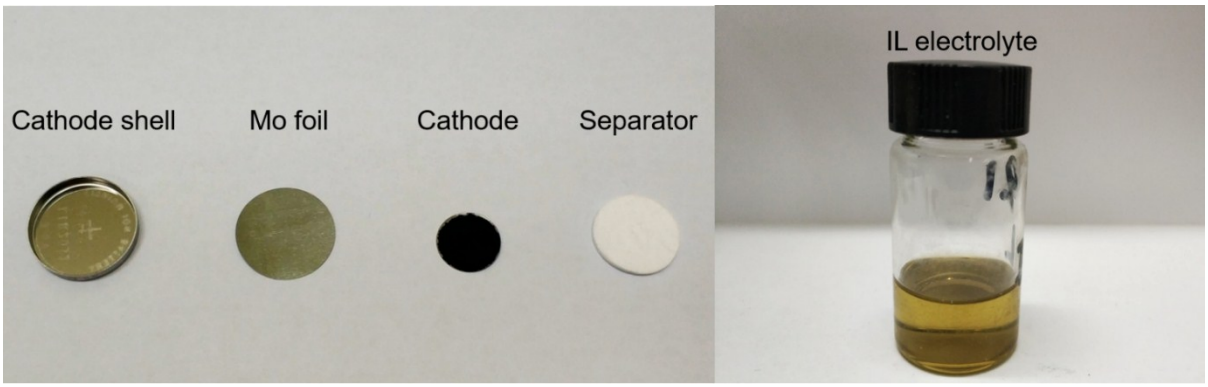

Fig. S2 Photograph of coin cell components. From left to right: cathode shell, Mo foil, cathode, separator, and IL electrolyte.

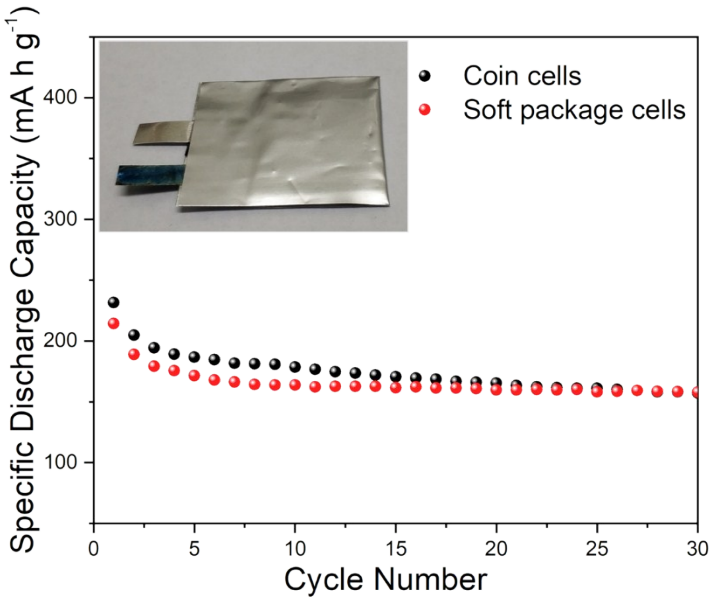

Fig. S3 Specific discharge capacities of coin cells and soft package cells at 500 mA g^{-1}.

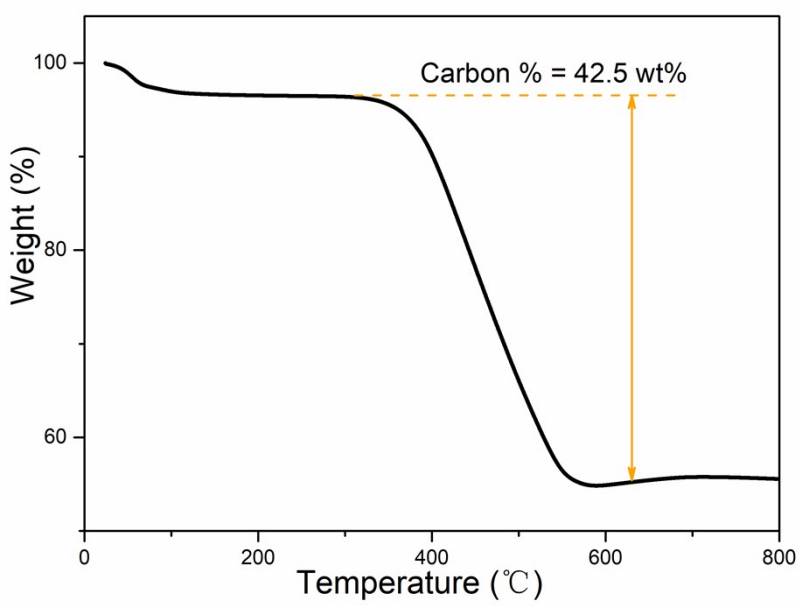

Fig. S4 TGA of the as-prepared SnO_2/C powder. The TGA measurement was performed under air atmosphere with a heating rate of 10 ℃ min^{-1}. The weight ratio of the carbon in the SnO_2/C nanocomposite is calculated to be 42.5 wt%.

a

Brookhaven Instruments

Summary Statistics Report

Type	Sample ID	Eff. Diam. (nm)	Sample ID	Eff. Diam. (nm)
DLS	SnO2 - 1	2,571.82	SnO2/C - 1	327.57
	SnO2 - 2	2,527.42	SnO2/C - 2	327.47
	SnO2 - 3	2,591.12	SnO2/C - 3	323.33
Sum	Mean:	2,563.45	Mean:	326.13

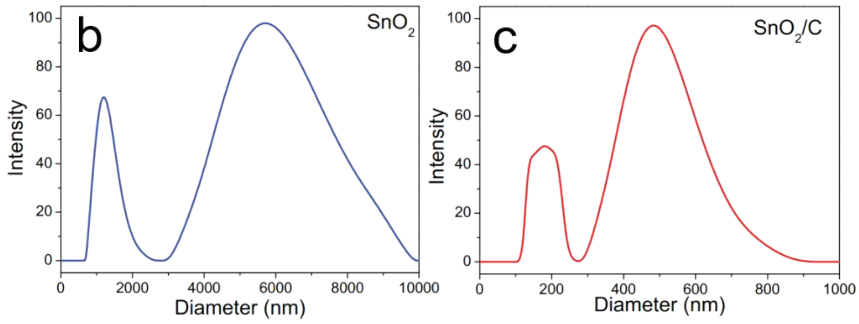

Fig. S5 a) Particle size statistics report for the as-prepared SnO_2 and SnO_2/C powder. b,c) Particle size distributions by intensity of the SnO_2 and SnO_2/C powder.

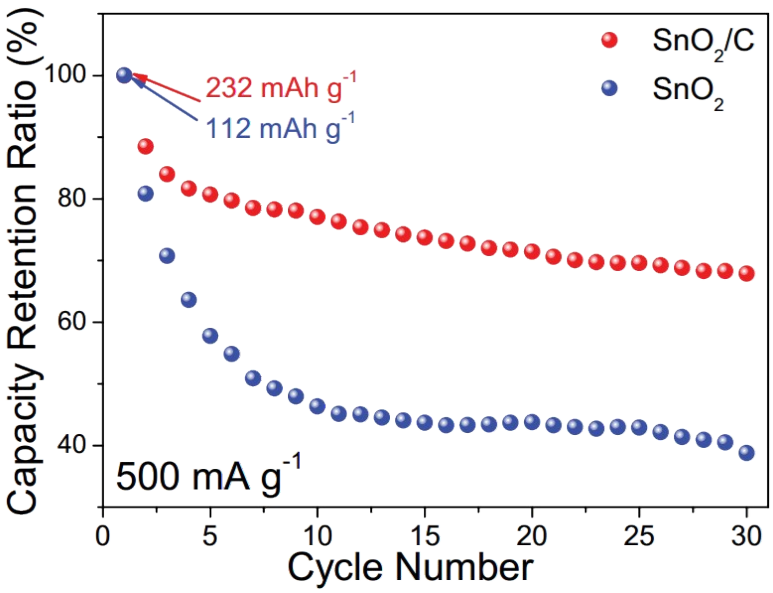

Fig. S6 Discharge capacity retention of SnO_2 and SnO_2/C cells within a voltage window of 0.05~1.95 V vs. Al/Al^{3+} at a current density of 500 mA g^{-1}. The discharge capacity retention of SnO_2 and SnO_2/C were 67.8% and 39% after 30 cycles, respectively. SnO_2/C performs much better than SnO_2 both in cycling stability and discharge capacities.

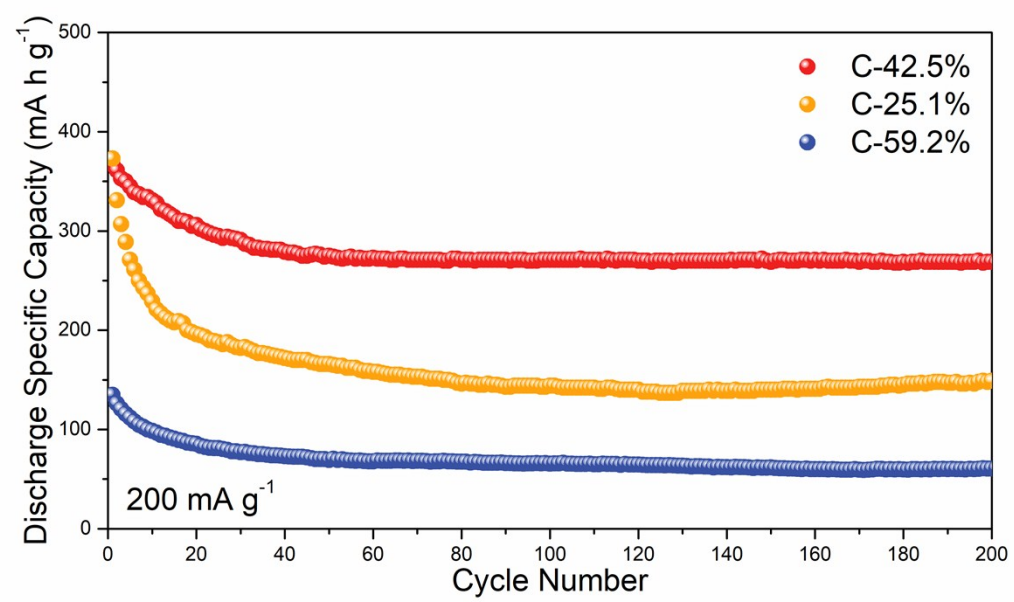

Fig. S7 Discharge specific capacities of SnO_2/C cells with different carbon content within a voltage window of 0.05~1.95 V vs. Al/Al^{3+} at a current density of 200 mA g^{-1}. The results suggest that insufficient carbon content leads to poor cycling stability, while excessive carbon content decreases the discharge capacity, moderate carbon content is conducive to improve the stability and discharge capacity of the cells.

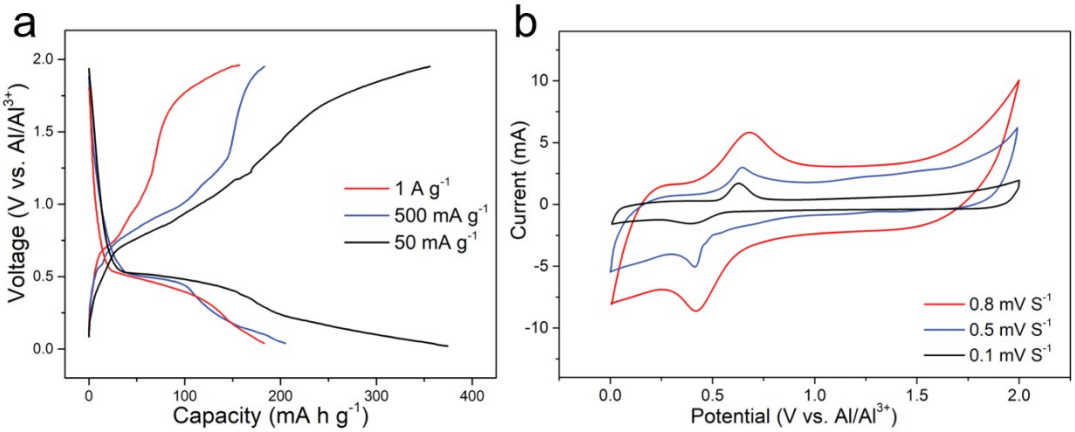

Fig. S8 Charge/discharge voltage profiles of different current densities and CV curves of the third cycles at different scan rates.

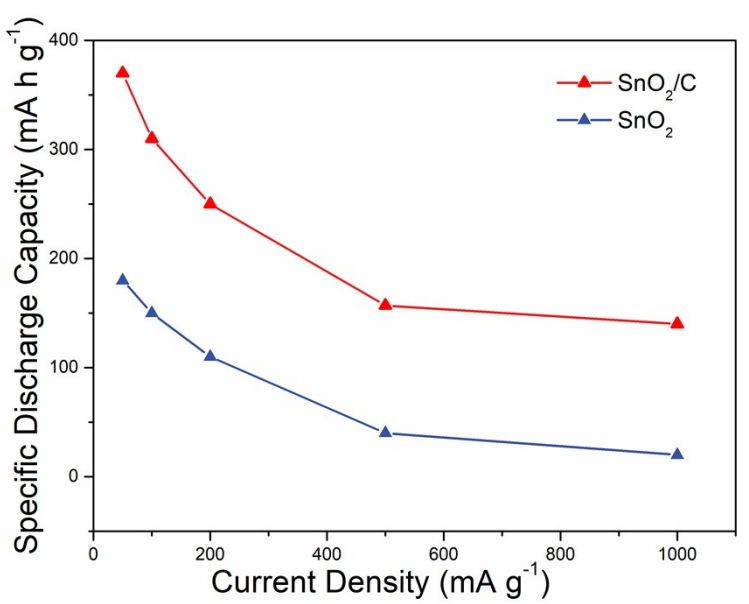

Fig. S9 Stabilized specific discharge capacities of SnO_2 and SnO_2/C cells at different current densities. The 50th discharge specific capacities at different current densities were used. It is revealed in the body of the article that the discharge capacities of the cells regained stability after 10th cycle due to the stabilization of side reactions. The SnO_2/C undergoes a high stabilized discharge capacity of 370 mA h g^{-1} compared with 180 mA h g^{-1} of the SnO_2 at a current density of 50 mA g^{-1}. Even at a high current density of 1 A g^{-1}, the discharge capacities of SnO_2/C could remain 140 mA h g^{-1}, while there is only 20 mA h g^{-1} left in the SnO_2.

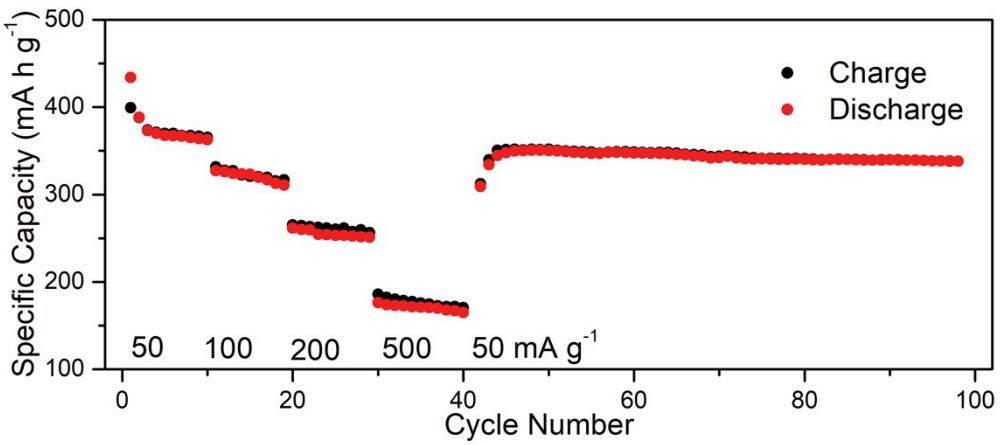

Fig. S10 The rate performance of SnO_2/C cathode at various current densities ranging from 50 to 500 mA g^{-1}. As shown, SnO_2/C cells deliver a stabilized discharge capacity of 370, 310, 250, 157 mA h g^{-1} at current densities of 50, 100, 200, 500 mA g^{-1}, respectively. In addition, the discharge capacity can recover to 350 mA h g^{-1} when change the current density from 500 mA g^{-1} back to 50 mA g^{-1}.

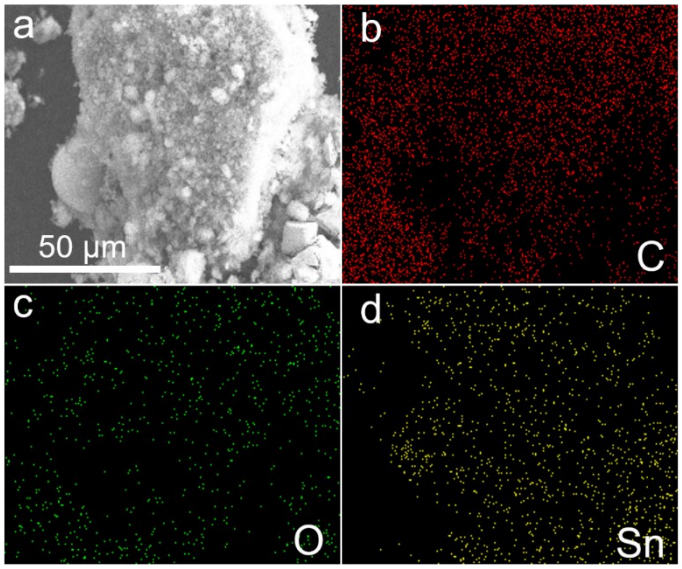

Fig. S11 SEM image and element mapping images of SnO_2/C powder. The images show the uniform distribution of C, O and Sn all over the SnO_2/C nanocomposite.

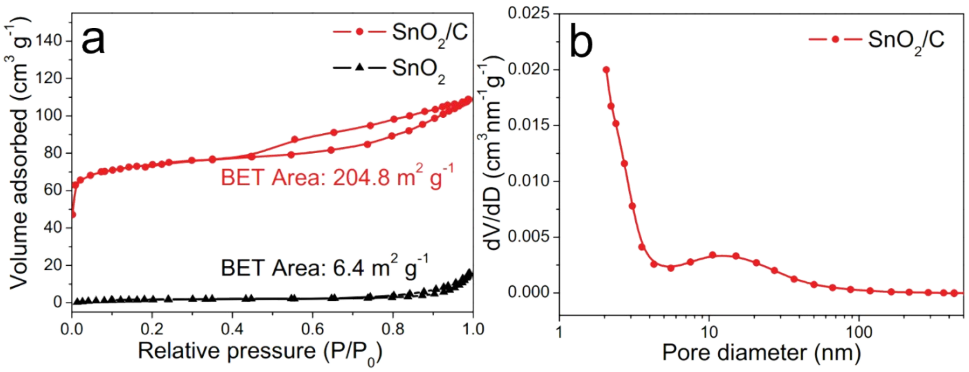

Fig. S12 a) N_2 adsorption-desorption isotherms of the SnO_2 and SnO_2/C powder. The BET specific surface area is 6.4 m^2 g^{-1} for SnO_2 and 204.8 m^2 g^{-1} for SnO_2/C. The specific surface area of the SnO_2/C is 32 times larger than that of the SnO_2. b) Pore-size distribution of SnO_2/C powder.

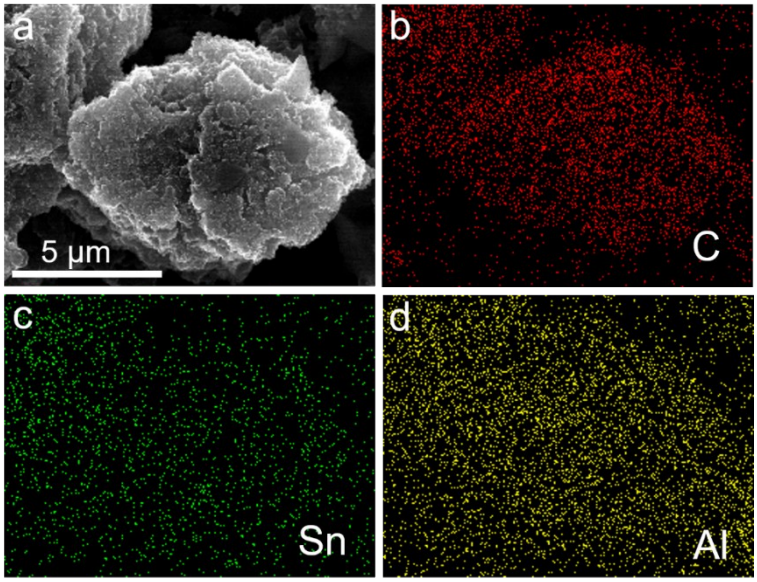

Fig. S13 SEM image and element mapping images of SnO_2/C cathode at fully discharge state. As shown, a large amount of Al exists in the cathode, indicating the insertion of Al^{3+} into the cathode.

According to the Bragg's Law:

$$2dsin\theta = n\lambda$$

Where d represents the lattice spacing, θ is the angle between the incident ray, the reflected ray and the reflecting surface, n represents the reflection series, and λ is the wave length of the X-ray (λ = 1.5405 Å). As shown in Supplementary Table 1, the slight 2θ shift reflects to only ~ 0.01 Å change in the lattice spacing.

Table S1. Lattice spacing calculated by Bragg's Law.

2theta / °	**lattice spacing / Å (calculated)**	**lattice plane**
26.6 (pristine)	3.348	(110)
26.5 (cycled)	3.361	(110)
33.9 (pristine)	2.642	(101)
33.8 (cycled)	2.650	(101)

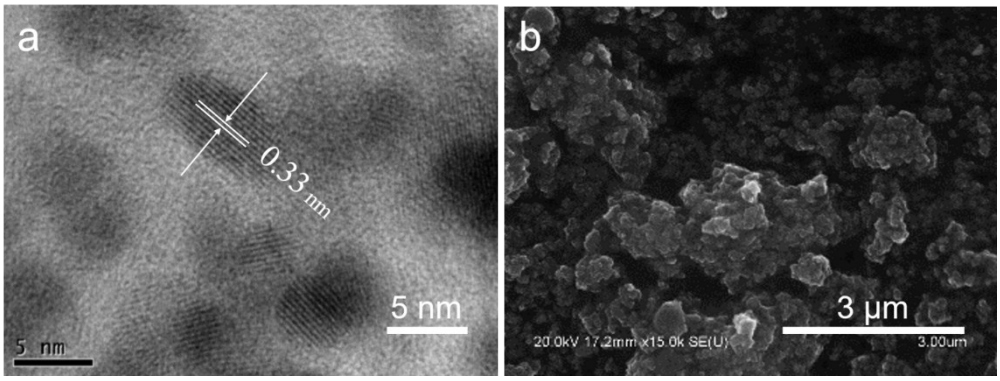

Fig. S14 a) HRTEM and b) SEM images of the SnO_2/C electrodes under fully discharge state after 20,000 cycles.

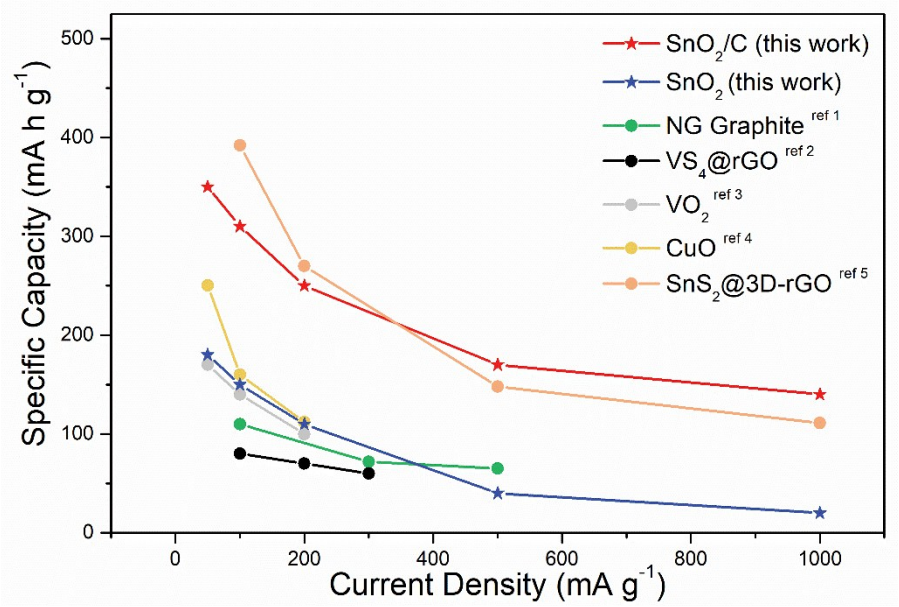

Fig. S15 Rate performances of SnO_2/C and other representative AIB cathode materials. SnO_2/C cells exhibit large discharge capacities among the investigated AIB cathodes.

Table S2. Cycling performance of SnO_2/C and other AIBs cathode materials.

Cathode	Cycle number	Current density (mA g^{-1})	Specific discharge capacity (mA h g^{-1})
SnO_2/C this work	16,000	2,000	72
	1,100	1,000	140
NG graphite ref 1	6,000	60	60
VS_4@rGO ref 2	100	100	80
		200	70
		300	60
VO_2 ref 3	100	50	116
CuO ref 4	100	50	130
		100	121
		200	112
SnS_2@3D-rGO ref 5	100	1000	112

References

1. D. Y. Wang, C. Y. Wei, M. C. Lin, C. J. Pan, H. L. Chou, H. A. Chen, M. Gong, Y. Wu, C. Yuan, M. Angell, Y. J. Hsieh, Y. H. Chen, C. Y. Wen, C. W. Chen, B. J. Hwang, C. C. Chen and H. Dai, *Nat. Commun.*, 2017, **8**, 14283.
2. X. Zhang, S. Wang, J. Tu, G. Zhang, S. Li, D. Tian and S. Jiao, *ChemSusChem*, 2018, **11**, 709-715.
3. W. Wang, B. Jiang, W. Xiong, H. Sun, Z. Lin, L. Hu, J. Tu, J. Hou, H. Zhu and S. Jiao, *Sci. Rep.*, 2013, **3**, 3383.
4. X. Zhang, G. Zhang, S. Wang, S. Li and S. Jiao, *J. Mater. Chem. A*, 2018, **6**, 3084-3090.
5. Y. Hu, B. Luo, D. Ye, X. Zhu, M. Lyu and L. Wang, *Adv. Mater.*, 2017, **29**.